Identification of Human Vesicle Monoamine Transporter (VMAT2) Lumenal Cysteines That Form an Intramolecular Disulfide Bond†

David S. Thiriot, Michael K. Sievert, and Arnold E. Ruoho*

Department of Pharmacology, University of Wisconsin−Madison Medical School, 1300 University Avenue, Madison, Wisconsin 53706-1532

Received September 18, 2001; Revised Manuscript Received March 28, 2002

ABSTRACT: The vesicle monoamine transporter (VMAT2) concentrates monoamine neurotransmitter into synaptic vesicles. To obtain structural information regarding this large membrane protein by analysis of disulfide bonds and other intramolecular cross-links, we engineered a strategic thrombin cleavage site into deglycosylated, HA-tagged human VMAT2. Insertion of this protease site did not disrupt ligand binding or serotonin transport. Thrombin cleavage at an engineered site in the predicted cytoplasmic loop between transmembrane (TM) domains 6 and 7 (loop 6/7) was rapid and quantitative in the absence of any detergent. The loop 6/7 thrombin site allowed assessment of an intramolecular disulfide bond between the N- and C-terminal halves of the transporter. Consistent with this hypothesis, after quantitative loop 6/7 thrombin cleavage, in the absence of reducing agent, VMAT2 migrated on SDS−polyacrylamide gels as a full-length transporter. Addition of dithiothreitol resulted in complete conversion from full-length to thrombin-cleaved size, demonstrating a DTT-reversible covalent bond. The identity of the disulfide-bound cysteine pair was suggested by the observation that replacement of Cys 126 or Cys 333 with serine both reduced [^{3}H]serotonin transport. Replacement of either Cys 126 or Cys 333 was found to eliminate the DTT-reversible intramolecular covalent bond. We conclude that human VMAT2 Cys 126 in loop 1/2 and Cys 333 in loop 7/8 form a disulfide bond which contributes to efficient monoamine transport.

The vesicle monoamine transporter (VMAT2)[1] is a proton monoamine antiporter which concentrates monoamine neurotransmitters into synaptic vesicles. VMAT2 transports a wide range of substrates including serotonin, dopamine, and norepinephrine and is inhibited by a number of drugs including reserpine, tetrabenazine (TBZ), and ketanserin. From the initial VMAT biochemical purification (*1*) and cloning of neuronal and endocrine isoforms (*2*, *3*) to studies of knockout mice (*4*−*6*) and intracellular trafficking (*7*), VMAT has provided important new insights into monoaminergic neuronal function. This has included suggestions of potential clinical contributions to psychiatric (*8*) and heart disorders (*5*, *9*) and drug abuse (*5*, *6*). Some aspects of VMAT2 biology and physiology have been recently reviewed (*8*, *10*, *11*).

On the basis of amino acid sequence, the prediction is that VMAT2 contains 12 transmembrane (TM) helices, a structural commonality with a number of other transporters including plasma membrane monoamine reuptake transporters and P-glycoprotein. Mutagenesis and chimera experiments (*12*−*17*) have suggested important residues which may contribute to ligand binding and monoamine transport. Our recent demonstration of a ligand-protectable MTSEA-reactive cysteine in TM 11 (Cys 439) (*18*) strengthens and extends some of these conclusions. In addition, two significant observations which have contributed to VMAT2 structural information are the discovery that a lysine in predicted TM 2 and an aspartate in predicted TM 11 interact functionally as an ion pair (*19*) and the identification from photoaffinity labeling studies performed in our laboratory (*20*, *21*) of two distinct photoinsertion sites for TBZ- and ketanserin-based photolabels, suggesting a juxtaposition of TM 1 with TM 10/11. While the reasonable inferences from molecular biology and the biochemical structural information from photoaffinity labeling have provided significant and novel information, a more general approach which can be applied to obtain structural information for the entire molecule has been sought.

Biochemical demonstration of naturally occurring disulfide bonds, or alternatively of cross-links between engineered cysteines, has proven a powerful approach to obtain structural information about large transmembrane proteins. In addition to the well-characterized disulfide bond identified in rhodopsin (*22*), a few notable examples of receptors and transporters for which natural or engineered disulfides have been identified or suggested include the β_2-adrenergic receptor (*23*−*25*), lactose permease (*26*, *27*), the plasma membrane serotonin transporter (*28*, *29*), P-glycoprotein (*30*), and the Tn10 metal tetracycline proton antiporter (*31*, *32*).

† This work was supported by NIH Grant R01 NS33650 to A.E.R. D.S.T. received support from an NIH chemistry/biology interface predoctoral training grant and from a Pharmaceutical Research and Manufacturers of America (PhRMA) Foundation advanced predoctoral fellowship.

* To whom correspondence should be addressed. E-mail: aeruoho@facstaff.wisc.edu. Phone: (608) 263-5382. Fax: (608) 262-1257.

[1] Abbreviations: VMAT, vesicle monoamine transporter; TM, transmembrane; TBZ, tetrabenazine; ^{3}H-TBZOH, [^{3}H]dihydrotetrabenazine; G-HA, glycosylation minus, HA epitope; MTSEA, methanethiosulfonate−ethylamine; NEM, *N*-ethylmaleimide; DTT, dithiothreitol.

10.1021/bi015779j CCC: $22.00
Published on Web 04/26/2002

To test whether a naturally occurring disulfide bond is present in human VMAT2, a thrombin cleavage site was strategically placed into the cytoplasmic loop between predicted TM 6 and 7 of human VMAT2. This inserted thrombin site was shown not to disrupt native function and to be readily cleavable by thrombin. By comparing the electrophoretic mobility of quantitatively thrombin-cleaved WT and cysteine-replacement human VMAT2 constructs in the presence and absence of reducing agent, we report the presence of a disulfide bond in human VMAT2 between Cys 126 in the lumenal loop between TMs 1 and 2 (loop 1/2), and Cys 333 in the lumenal loop between TMs 7 and 8 (loop 7/8). Assay of [^{3}H]serotonin transport in transporters lacking Cys 126 or Cys 333 demonstrates that this disulfide bond contributes to efficient monoamine transport into vesicles.

EXPERIMENTAL PROCEDURES

Materials. The following materials used in this research were from the indicated sources (in parentheses): plasmid pCDNA 3.1 (Invitrogen, Carlsbad, CA), mutagenic and sequencing oligonucleotides (Integrated DNA Technologies, Coralville, IA), spin miniprep and large-scale plasmid DNA preparation kits (Qiagen, Valencia, CA), Amplitaq FS and Big Dye DNA sequencing reagents (Perkin-Elmer, Boston, MA, through the University of Wisconsin Biotechnology Center), COS-7 or -7L cells (ATCC, Manassas, VA; Life Technologies, Rockville, MD), restriction enzymes (New England Biolabs, Beverly, MA), Pfu DNA polymerase (Stratagene, La Jolla, CA), DMEM, penicillin/streptomycin/glutamine, Fungizone, cell culture trypsin, and PBS (Life Technologies, Rockville, MD), sodium [^{3}H]borohydride and [^{3}H]serotonin (NEN, Boston, MA), tetrabenazine (Fluka, Milwaukee, WI), methanethiosulfonate−ethylamine (Toronto Research Chemicals, North York, Ontario, Canada), anti-HA and anti-Myc antibodies (Covance Research Products, Denver, PA), polyethylenimine, ATP, 2-mercaptoethanol, *N*-ethylmaleimide (NEM), and dithiothreitol (DTT) (Sigma, St. Louis, MO), thrombin (Roche Molecular Biochemicals, Indianapolis, IN), goat anti-mouse HRP antibody, 0.4 cm gap width electroporation cuvettes, 12% Tris−glycine precast electrophoresis ready gels, Laemmli SDS sample buffer, and prestained molecular weight markers (Bio-Rad, Hercules, CA), Supersignal chemiluminescent substrates and Superblock PBS blocking buffer (Pierce, Rockford, IL), hyperfilm ECL (Amersham-Pharmacia, Piscataway, NJ), GF/B filter disks (Whatman through Fisher, Hanover Park, IL), Whatman GF/B filter sheets (Brandel, Gaithersburg, MD), transfection-competent *Escherichia coli* (Stratagene, La Jolla, CA; Novagen, Madison, WI), and emulsifier safe scintillation cocktail (Packard, Meriden, CT). Others reagents (sucrose, HEPES, KCl, $MgSO_4$, NaOH, KOH, Tris, additional restriction enzymes, etc.) were from reputable and readily available sources.

Construction of the Human VMAT2 Protease Site and Cysteine Replacement Mutants. A cDNA encoding human VMAT2 was the kind gift of Dr. Robert H. Edwards (UCSF School of Medicine, San Francisco, CA). The construction, subcloning, and functional testing of C-terminal FLAG- and 6-histidine-tagged human VMAT2 were previously reported (*18*). (All human VMAT2 constructs used in this research were derived from the C-terminal FLAG- and 6-histidine-tagged construct, which hereafter will be referred to as "WT".) For Western blots, the constructs used incorporated a set of four glycosylation site mutations and an HA epitope tag, collectively referred to as "G-HA", for "glycosylation minus, HA epitope", which were previously described (*18*). The thrombin site was added in predicted loop 6/7 by the QuickChange method (Stratagene) using native Pfu polymerase, *Dpn*I, and XL-10 gold supercompetent cells. The forward strand of the mutagenic oligo had the following sequence: 5′-GTGCTCCAGCCGTCCCGGGTGCTAGT-ACCACGAGGATCCCAGCCAGAGAGTCAGAAG-GGGACACC-3′, which placed the thrombin protease site (LVPRGS) between Val 275 and Gln 276 of human VMAT2. Replacements of Cys 126 with serine, and Cys 333 with serine or alanine, were performed by either the GeneEditor (Promega) or QuickChange (Stragatene) mutagenesis methods, using mutagenic oligos as follows: Cys 126 Ser, 5′-GCTGTTCCTTCCGACTCACCCAGTGAA GA-CAAAGACC-3′ (and complement); Cys 333 Ser, 5′-CCACTTTCGGGAGCTCATGGTCTCCATCATCC-3′ (a reverse strand primer); Cys 333 Ala, 5′-GGATGATG-GAGACCATGGCTAGCCGAAAGTGGCAGCTGG-3′ (and complement). All constructs were confirmed by DNA sequencing.

Transient Expression and Harvesting from COS-7 Cells. DNA purification, cell culture, and transient transfection were performed in all essential respects as previously described (*18*). Briefly, confluent 150 mm plates of COS cells were harvested and transfected by electroporation (in 0.4 cm gap width cuvettes with the voltage of the Bio-Rad genepulser/capacitance extender unit set at 0.226 mV and the capacitance set at 0.950 μF) with 15−50 μg of purified maxiprep or miniprep plasmid DNA (an equal amount for all constructs within a given experiment). Cells were harvested 1.5−4 days posttransfection, the cell culture medium usually being changed once within that time period. Cells were detached with trypsin, washed with buffer, and homogenized with a custom-built steel ball homogenizer, or "cell cracker" (*33*). After passage through the cell cracker approximately 30 times, the homogenate was centrifuged for 5 min at 735*g*, and the vesicle containing supernatant was collected for use in functional assays or Western blots. When the membranes were intended for use in ligand binding or uptake assays, COS cells were homogenized in the presence of protease inhibitor buffer containing 20 μg/mL leupeptin, 100 μM PMSF, 100 μM benzamidine, and 10 μg/mL soybean trypsin inhibitor. When the membranes were intended for proteolysis reactions and Western blots, transfected COS cells were homogenized in 0.3 M sucrose/10 mM HEPES, pH 7.2, in the absence of protease inhibitors and stored frozen at −20 to −80 °C. Occasionally (as indicated in the figure legends), COS homogenates were further subjected to ultracentrifugation, and the pellet was resuspended (with shearing through a small gauge needle) in 0.3 M sucrose/10 mM HEPES for use in Western blots. (In terms of background anti-HA immunoreactivity, Western blots of total COS homogenate are similar to Western blots using the high-speed membrane pellet fraction only.) Protein concentrations of COS vesicle preparations were assessed by the Bradford method using the Bio-Rad protein assay reagent by comparison to standard curves of bovine serum albumin. Generally, duplicate readings of triplicate samples were used to measure protein concentrations.

^{3}H-TBZOH Ligand Binding and [^{3}H]Serotonin Uptake Assays. Synthesis of the high-affinity VMAT2 radioligand [^{3}H]dihydrotetrabenazine (^{3}H-TBZOH) was performed as previously described (*18*). Ligand binding curves were performed by incubation of 50 μL of COS homogenate (134−160 μg) with 200 μL of 0.3 M sucrose/10 mM HEPES (pH 7.2) buffer containing the ^{3}H-TBZOH. Binding curves were derived from measurements at eight different concentrations of ^{3}H-TBZOH in the range of 1−46 nM. Specific binding was assessed by addition of excess nonradioactive TBZ (approximately 50 μM). In addition to some non-TBZ-protectable binding, it was found that nontransfected COS cells themselves have a low level of "specific", or TBZ-protectable, ^{3}H-TBZOH binding. This was controlled for by performing parallel analysis of mock-transfected COS cells (electroporated with no DNA added) and subtracting the low level of specific binding. Ligand binding at 30 °C was allowed to proceed for >20 min. Monoamine uptake experiments were performed by incubation at 30 °C of 50 μL of COS homogenate in the presence or absence of approximately 50 μM tetrabenazine (TBZ) (or, if indicated in the figure legend, 5 μM of the proton ionophore FCCP, which inhibits transport to the same extent) with 200 μL of buffer (sucrose/HEPES/protease inhibitors/ATP and salts) for final concentrations of 50 nM [^{3}H]serotonin, 5 mM ATP, 5 mM $MgSO_4$, and 4 mM KCl. From time course studies, 3 min was considered to be in the initial rate linear range, and steady-state accumulation was reached by times shortly after 5 min. Human VMAT-containing COS vesicles with bound ^{3}H-TBZOH or accumulated [^{3}H]serotonin were collected on GF/B filters by vacuum filtration on Millipore 12-well filtration manifolds or on a Brandel M-48 BIT cell harvester. Uptake assays which were vacuum filtered on the Millipore manifolds were performed in glass test tubes, and the test tubes were generally rinsed with 2 × 4 mL of buffer (which was also vacuum filtered). Assays filtered using the Brandel cell harvester were performed in 1.2 mL well volume polypropylene 96-well plates, and the wells were rinsed with 5 × 1 mL of buffer. Radioactivity was quantitated by scintillation counting in a Packard Model 1600CA or 2000CA scintillation counter.

Proteolysis Reactions with Thrombin. Proteolysis reactions with thrombin were carried out for the times and at the temperatures indicated in the figure legends, in the range of 10 min to 1 h at 16−37 °C. The optimum pH for thrombin cleavage is reported by the supplier to be 8.2−9.0; however, successful cleavage reactions were carried out in a pH range of 7.2−8.9, as indicated in the figure legends. Lyophilized thrombin, which contains significant amounts of EDTA and citrate, was resuspended in water at an activity of 0.1 unit/μL. In control Western blots, an amount of thrombin (molecular mass 33.6 kDa) equivalent to the highest amount loaded in any experimental condition described in these studies does not show any anti-HA immunoreactivity (data not shown).

Western Blots. Protein samples of the amounts indicated in the figure legends were electrophoresed on 12% SDS−PAGE gels in the presence or absence of reducing agent, as indicated. Following electrophoresis, proteins were transferred to a 0.2 μM nitrocellulose membrane either for 1 h at 100 V or for 12 h at 30 V, in a buffer comprised of 25 mM Tris, 192 mM glycine, and 20% methanol (no SDS), pH 8.3. Nonspecific antibody binding sites were blocked by incubating the blot for 1 h or longer in Superblock PBS (Pierce) + 0.05% Tween-20. Anti-HA or anti-Myc antibody was diluted 1:850−1:1000 in 15 mL of Superblock/0.05% Tween and allowed to bind for 1 h or longer, followed by at least six washes of 5 min or longer with Tris-buffered saline (TBS)/0.05% Tween-20. The secondary antibody conjugate was goat anti-mouse HRP (Bio-Rad), diluted 1:50000 (or more) in 15 mL of Superblock/0.05% Tween, and was allowed to bind for at least 1 h, followed by a second set of 6 × 5 min washes in TBS/0.05% Tween. Pierce ECL reagents were used following the manufacturer's recommendations, and then the blots were imaged using hyperfilm ECL (Amersham Pharmacia).

Statistical Analysis and Graphing. Graphing, nonlinear curve fitting (K_d and B_{max} calculations), linear regressions for protein assays, and statistical analysis were performed using the computer program Prism (GraphPad, San Diego, CA). The statistical significance of observed effects was assessed on the basis of the scintillation counting data using this program by a two-tailed, unpaired *t*-test and is indicated in Figure 4 as follows: * = $p < 0.1$, ** = $p < 0.01$, *** = $p \leq 0.001$. Error bars show either the SEM or 95% confidence interval of multiple measurements, as specified in the figure legends.

RESULTS

Assessment of the Sensitivity of Human VMAT2 to Cleavage by Thrombin and Construction of Loop 6/7 Thrombin Site Human VMAT2. Thrombin recognizes the sequence L-V-P-R-G-S (cleaving between the R and G) and certain other similar sequences. Human VMAT2 does not contain a consensus recognition sequence for thrombin, nor any highly similar sequence. However, to ensure suitability for our purpose, we tested thrombin for its ability to proteolyze human VMAT2 at nonconsensus sequences. To facilitate detection by Western blot, a functional human VMAT2 construct was used to assess proteolysis in which the four consensus glycosylation sequences in the large lumenal loop (between TM 1 and TM 2) were mutated and an HA epitope was inserted (Figure 1B). This set of four glycosylation site mutations and insertion of an HA epitope are together referred to throughout this paper as G-HA, for glycosylation minus, HA epitope, as previously described (*18*). As demonstrated in Figure 1A, membrane-bound human VMAT2 from total COS cell homogenate is resistant to cleavage by thrombin in the absence of added detergent. (The thrombin used in this experiment was freshly purchased and confirmed to be functionally active in separate experiments on a control thrombin site-containing fusion protein; data not shown.) Therefore, the thrombin recognition sequence appeared to be an ideal candidate for use as an engineered protease site.

The normal electrophoretic mobility of WT G-HA VMAT2 on a 12% Tris−glycine SDS−PAGE gel (compared with Bio-Rad molecular mass standards, catalog no. 1610318) is clearly demonstrated in Figure 1A to be slightly below the 51 kDa molecular mass marker, with a much smaller amount migrating at the predicted size (based on primary sequence) of 58 kDa. Surprisingly, the addition of thrombin results in a shift to higher molecular mass, reflected in partial conversion of the 50−51 kDa band to the 58 kDa band (the

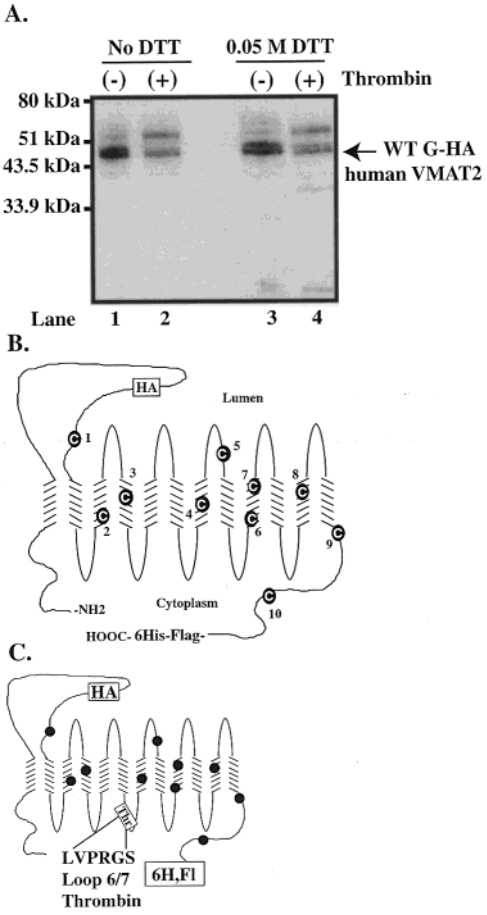

FIGURE 1: An engineered thrombin cleavage site in a predicted human VMAT2 loop region. (A) Sensitivity of HA-tagged, deglycosylated human VMAT2 (WT G-HA) to cleavage by thrombin in the absence of added detergent. The set of mutations referred to collectively as G-HA has been previously described (*18*). Shown is an anti-HA Western blot of an SDS−PAGE gel loaded with equal amounts (approximately 45 μg) of COS homogenate pellet per lane, resuspended from a 10 min, 200000*g* centrifugation. In lanes 2 and 4, thrombin (0.4 unit, Roche catalog no. 602400) was added to the membranes in sucrose/HEPES buffer (pH 7.2) for 30 min at room temperature. Samples in lanes 1 and 2 were not treated with reducing agent prior to SDS−PAGE, while samples in lanes 3 and 4 were treated with 0.05 M DTT. (B) Positions of the 10 cysteines in the proposed secondary structure of WT G-HA VMAT2. As shorthand throughout this paper, cysteines are referred to by number as indicated in this figure. (C) Position of the engineered thrombin cleavage site in the proposed secondary structure of WT G-HA human VMAT2. The black circles represent the 10 cysteines, as indicated in panel B.

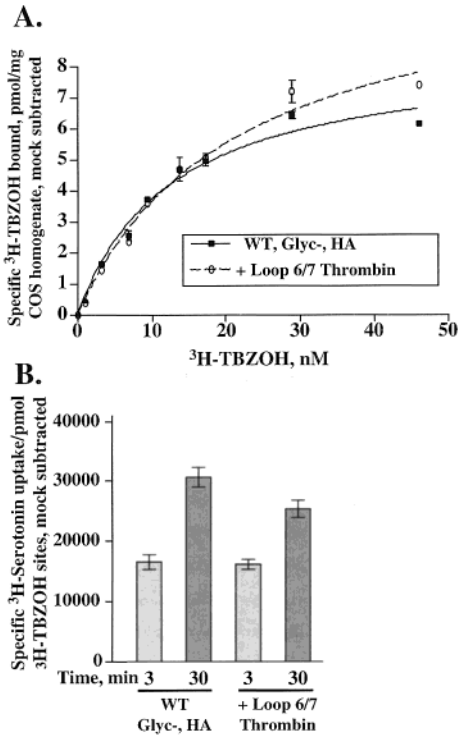

FIGURE 2: Loop 6/7 engineered thrombin site construct retains high-affinity ligand binding and serotonin transport. (A) ^{3}H-TBZOH binding curves for WT G-HA human VMAT2 and loop 6/7 thrombin site construct, demonstrating comparable ligand binding affinities and expression levels of native (ligand binding competent) transporters. Error bars show SEM of multiple measurements. (B) [^{3}H]Serotonin uptake by WT G-HA human VMAT2 and the loop 6/7 thrombin site construct, demonstrating that transport function is retained after addition of the thrombin cleavage site. Error bars show 95% confidence intervals of multiple measurements.

predicted size; see Figure 1A, lanes 2 and 4). Since thrombin itself shows no anti-HA immunoreactivity, and a similar shift is seen after addition of EDTA, the upper (58 kDa) band appears to result from chelating reagents present in commercially available thrombin. While an interesting phenomenon, the presence of this doublet does not alter the conclusions reached in these studies.

The positions of the 10 cysteines in human VMAT2 and of the two engineered thrombin sites are shown in Figure 1B,C. Throughout this paper, human VMAT2 cysteines will be referred to by their order number from the N- to C-terminus, as indicated in Figure 1B. The position for the engineered thrombin sequence was selected on the basis of examination of VMAT2 loop sequences from multiple organisms and identification of a region of higher sequence variation. The thrombin site between TM 6 and TM 7 (loop 6/7) was inserted between Val 275 and Gln 276.

Functional Testing of Loop 6/7 Thrombin Site Constructs. To confirm that insertion of the thrombin cleavage sequence did not disrupt the native conformation of human VMAT2, ligand binding affinity and monoamine transport were assayed and compared with WT G-HA human VMAT2. As seen in Figure 2A, the thrombin site construct retains high-affinity ^{3}H-TBZOH binding, with K_d values that differed from WT G-HA human VMAT2 by less than 2-fold. Similarly, [^{3}H]serotonin uptake at both short (linear range) and longer (steady-state accumulation) time points was similar to uptake by WT G-HA (Figure 2B). These data suggest that insertion of the thrombin recognition sequence does not disrupt native structure and that this thrombin site construct is suitable for use in biochemical structural studies.

Demonstration of a DTT-Reversible Covalent Bond between the N- and C-Terminal Halves of Loop 6/7 Thrombin Site Cleaved Human VMAT2. The availability of a unique proteolysis site which separates human VMAT2 into two halves allowed testing the hypothesis that a disulfide bond exists between the two halves of the molecule. Human VMAT2 contains three cysteines N-terminal of the loop 6/7 engineered thrombin cleavage site (refer to Figure 1C), and the remaining seven cysteines are C-terminal to the loop 6/7 thrombin site. If the hypothesis is correct that a disulfide bond exists between a cysteine on the N-terminal side of the thrombin site (Cys 1, 2, 3) with a cysteine C-terminal to

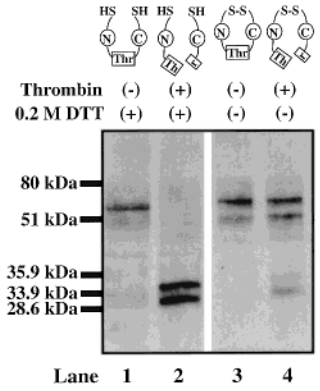

FIGURE 3: A covalent bond holds the two halves of thrombin-cleaved human VMAT2 together and is DTT reversible. Anti-HA Western blot of loop 6/7 thrombin site G-HA human VMAT2 (−) and (+) thrombin, in the presence and absence of reducing agent (200 mM DTT). Each lane was loaded with 13.6 μg of total COS homogenate. Aliquots containing 242 μg of total COS homogenate were incubated at 30 °C for 30 min (pH 8.0) and then cleaved with 0.8 thrombin unit (Roche) for 15 min at 30 °C, pH 8.0. Lanes 1 and 3 were loaded with the exact same sample, the only difference being the addition of DTT to lane 1. Lanes 2 and 4 were loaded with the exact same sample, the only difference being the addition of DTT to lane 2, demonstrating that the material blotting as full length in lane 4 had been quantitatively cleaved by thrombin. The diagrams above the Western blot lanes illustrate the two covalent linkages between the N- and C-terminal halves of the protein. One linkage (the VMAT2 peptide chain itself) is broken by cleavage with thrombin at the loop 6/7 engineered site. The other linkage is a DTT-reversible covalent bond (i.e., disulfide).

the thrombin site (Cys 4, 5, 6, 7, 8, 9, 10), then, in the absence of reducing agent, VMAT2 (containing a loop 6/7 thrombin site) would be expected to migrate and appear as full length on Western blot, despite thrombin cleavage at the loop 6/7 site. Further, this full-length band would be expected to disappear, with the concomitant appearance of the HA-tagged N-terminal half, simply upon reduction by DTT.

As demonstrated in Figure 3, the hypothesis for a disulfide bond between the two halves of human VMAT2 is supported. Human VMAT2 was detected by SDS−PAGE and Western blot as the full-length molecule in the presence of DTT, with no thrombin added (Figure 3, lane 1). Addition of thrombin for short periods of time (10−30 min) resulted in quantitative cleavage of the loop 6/7 site and appearance of the HA-tagged N-terminal half doublet (Figure 3, lane 2). In the absence of thrombin and DTT, VMAT2 Western blots as the full-length molecule (Figure 3, lane 3). However, after thrombin cleavage, but without added reducing agent, approximately 90% of the VMAT2 remained tethered together and appeared as the full-length molecule (Figure 3, lane 4). A faint band at the predicted position of the cleaved fragment as seen in Figure 3, lane 4, is reproducibly present, indicating that 5−10% of the transporters lack the disulfide bond. The membranes loaded in lane 4 were an aliquot from the same sample loaded in lane 2, the only difference being addition of DTT to the aliquot loaded in lane 2. Therefore, despite demonstrated quantitative cleavage by thrombin (lane 2) at the loop 6/7 site, the two halves of the molecule remained tethered together (lane 4) by a DTT-reversible covalent bond. These results have been repeated numerous times under varying conditions, including at lower temperatures and near neutral pH (data not shown), and with multiple different sets of transfected COS cell membranes. Importantly, NEM was added to a concentration >30 mM prior to addition of SDS sample buffer to ensure that the disulfide bond was not forming in the denatured molecule during the time period after addition of SDS. Sulfhydryl reagents have been added at (and within seconds following) the addition of SDS sample buffer at concentrations as high as 20 mM MTSEA and 120 mM NEM without any change in this result, again confirming the existence of the disulfide bond.

Functional Effects of Cysteine Replacements Suggest a Candidate Cysteine Pair for the Disulfide Bond. The results obtained in Figure 3 demonstrating a DTT-reversible covalent bond strongly support the conclusion that a disulfide bond exists between two cysteines on opposite sides of the loop 6/7 thrombin cleavage site. The logical conclusion follows that the disulfide bond would be between one of the cysteines from the set Cys 1, 2, or 3, with the other cysteine from the set Cys 4−10. An initial indication of which cysteines might be involved was provided by functional data on the effects of cysteine replacements on [^{3}H]serotonin uptake. Compared to human VMAT2 with all 10 native cysteines, replacement of Cys 1 (Cys 126) or Cys 5 (Cys 333) with Ser led to significant reductions in [^{3}H]serotonin transport (Figure 4). The inhibitory effect of replacement of Cys 1 or Cys 5 was specific for the transport function, as we had previously demonstrated that replacement of these two cysteines individually or together did not alter the WT K_d for ^{3}H-TBZOH binding (*18*). As a control, replacement of the other two predicted non-TM cysteines together (Cys 9 and 10) with Ser does not inhibit [^{3}H]serotonin transport (but actually led to an increase over WT control levels; data not shown). The reduction in [^{3}H]serotonin transport by human VMAT2 lacking Cys 1 and Cys 5 is reproducibly observed at steady-state time points (Figure 4A) and also in the linear uptake time range of a construct lacking the four non-TM cysteines (Figure 4B). In this construct, the inhibitory effect of replacement of Cys 1 and Cys 5 was dominant over the enhancement of transport conferred by replacement of Cys 9 and 10. While future detailed kinetic studies should provide additional insight, these functional data suggested that the disulfide bond may involve Cys 1 and Cys 5. This also appeared to be a reasonable hypothesis, based on the fact that, for all other potential cysteine pairs which could lead to our observation of DTT-reversible covalent bond, one or both cysteines are predicted to be in transmembrane segments.

Replacement of either Cys 1 (Cys 126) or Cys 5 (Cys 333) Eliminates the Disulfide Bond. To test whether Cys 1 and Cys 5 are in fact the two cysteines which form the disulfide bond, loop 6/7 thrombin site G-HA human VMAT2 constructs with single cysteine replacements (Cys 1 Ser or Cys 5 Ala) were constructed. In each of these constructs, the net difference from the loop 6/7 thrombin site control construct is the replacement of an SH moiety with an OH or H. For each construct, the ability of full-length thrombin-cleaved transporter to remain tethered together in a DTT-reversible manner was assessed.

As demonstrated in Figure 5 by SDS−PAGE and Western blot, absence of full-length (51−58 kDa) transporter and the prominent presence of the thrombin-cleaved (31−33 kDa) transporter in lanes 4 and 6 under *nonreducing* conditions support the conclusion that replacement of either Cys 1 or

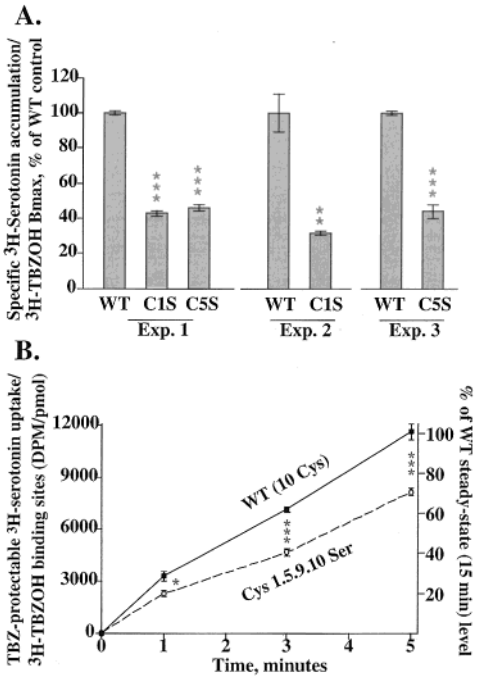

FIGURE 4: Functional effects of human VMAT2 cysteine replacements. The statistical significance of effects is indicated as described in Experimental Procedures. Error bars show the SEM of multiple measurements. (A) Comparison of specific [^{3}H]serotonin steady-state accumulation levels, normalized to the amount of high-affinity ^{3}H-TBZOH binding sites (B_{max} from ligand binding curves), between epitope-tagged WT human VMAT2 and the Cys 1 Ser or Cys 5 Ser replacement constructs. Uptake experiments were for 15 min at 30 °C and are plotted as percentage of WT [^{3}H]serotonin accumulation/^{3}H-TBZOH B_{max}. For experiments 1 and 3, specific uptake is defined as uptake protectable by approximately 50 μM TBZ. For experiment 2, specific uptake is defined as uptake protectable by 5 μM proton ionophore, FCCP. These concentrations of TBZ and FCCP inhibit WT human VMAT2 monoamine transport to the same extent (data not shown). (B) Time course of TBZ-protectable [^{3}H]serotonin uptake per amount of ^{3}H-TBZOH high-affinity binding sites, comparing WT VMAT2 and C1.5.9.10S VMAT2 (a construct in which the four predicted non-TM cysteines have been replaced by serines). Uptake is plotted verses time as [^{3}H]serotonin dpm/pmol of ^{3}H-TBZOH binding sites and as percentage of WT steady-state accumulation (WT uptake at 15 min).

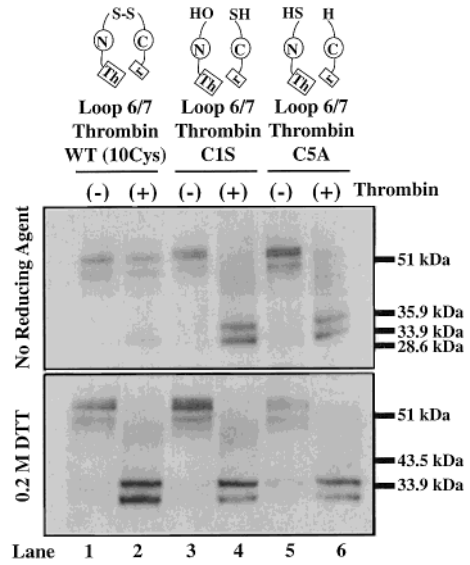

FIGURE 5: Elimination of the disulfide bond by replacement of either human VMAT2 Cys 1 (Cys 126) or Cys 5 (Cys 333). Anti-HA Western blot comparison of the electrophoretic mobility of thrombin-cleaved VMAT2 in the absence and presence of reducing agent (0.2 M DTT) between loop 6/7 thrombin constructs with all 10 cysteines (WT), Cys 1 Ser, or Cys 5 Ala. Samples of 177−215 μg of total COS homogenate were incubated with 20 mM EDTA, 20 mM EGTA, and 150 mM HEPES (pH 8.0) at 30 °C for 30 min, followed by addition of 0.8 unit of thrombin (or water) for 10 min at 30 °C. NEM was then added to a concentration of 32 mM, and the solution was incubated for 10 min at 30 °C, followed by addition of SDS sample buffer. Aliquots were divided, and DTT was added to 0.2 M for the reduced experimental condition. The upper blot is in the absence of reducing agent, and the lower blot is the same material with reducing agent added. Lanes 1 and 2: WT (−) and (+) thrombin, 21.5 μg of COS homogenate per lane. Lanes 3 and 4: C1S (−) and (+) thrombin, 21.5 μg of COS homogenate per lane. Lanes 5 and 6: C5A (−) and (+) thrombin, 17.7 μg of COS homogenate per lane. In lanes 4 and 6 of the upper blot (nonreduced condition), the relative lack of the full-length transporter and the prominent presence of cleavage product both indicate that replacement of either Cys 1 or Cys 5 eliminates the disulfide bond.

Cys 5 eliminated the DTT-reversible covalent bond which tethered the two halves of the molecule together. Full-length loop 6/7 thrombin-cleaved G-HA human VMAT2 remains covalently tethered in the absence of DTT, but Cys 1 Ser or Cys 5 Ala human VMAT2 does not. From these data we conclude that a disulfide bond exists between the two halves of the molecule involving Cys 1 (Cys 126) and Cys 5 (Cys 333).

DISCUSSION

To biochemically demonstrate the presence of a disulfide bond in human VMAT2, our approach was to show that, despite quantitative cleavage at a strategically engineered thrombin site between a cysteine pair forming a disulfide bond, human VMAT2 still migrated as full-length transporter as assessed by SDS−PAGE and Western blot in the *absence* of reducing agent (Figures 3 and 5). Addition of DTT reduced this disulfide bond, resulting in loss of the full-length band and appearance of the lower molecular mass cleaved band as assessed by Western blots (Figures 3 and 5). To succeed with this method, we required a human VMAT2 which would be cleavable at a unique site between the disulfide-bound cysteine pair. In the absence of detergent, human VMAT2 in COS vesicles is completely resistant to cleavage by thrombin (Figure 1A) and demonstrates little if any cleavage even in the presence of SDS (data not shown). (Although doublets of both full-length and fragments of VMAT2 are present under certain conditions, these doublets do not alter the conclusions reached in these studies.) Therefore, we chose to use the thrombin protease site and placed this sequence into human VMAT2 cytoplasmic loop 6/7, which divided VMAT2 roughly in two halves. The engineered thrombin site does not disrupt VMAT2 ligand binding or function (Figure 2), and can be quantitatively cleaved by thrombin without any added detergent (Figure 3).

The identity of the disulfide-bound cysteines was suggested from observation of the functional effects of Cys 1 and Cys 5 replacements on human VMAT2 [^{3}H]serotonin uptake. Replacement of either Cys 1 or Cys 5 with serine significantly reduced [^{3}H]serotonin accumulation at steady-state time points (Figure 4A) without changing the ^{3}H-TBZOH binding K_d (*18*). These replacements also have a dominant inhibitory effect on [^{3}H]serotonin uptake in a construct lacking the four non-TM cysteines (Cys 1, 5, 9,

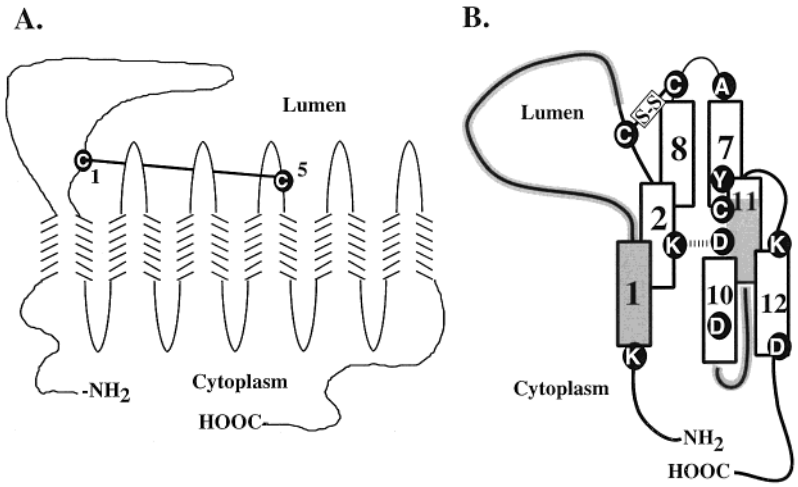

FIGURE 6: A model for human VMAT2 incorporating the Cys 1−Cys 5 disulfide bond and previously available experimental evidence. (A) Predicted 12 TM diagram of human VMAT2, indicating the position of the Cys 1−Cys 5 disulfide bond. (B) Hypothetical helix-packing model for TMs 1/2, 7/8, and 10−12, incorporating the Cys 1−Cys 5 disulfide bond and previously reported experimental data. TM 1−loop 1/2 and loop 10/11−TM11 photolabeled peptides (*20*) are filled or outlined in gray. (The lysine at the cytoplasmic interface of TM 1 is the primary photoinsertion site of the ketanserin-based photolabel, [^{125}I]azidoiodoketanserin.) The lysine in TM 2 and aspartate in TM 11 are reported to form an ion pair (*19*). MTSEA reaction at the cysteine in TM 11 results in inhibition of ^{3}H-TBZOH binding, protectable by preincubation with ^{3}H-TBZOH (*18*). The loop 7/8 alanine, TM 10 aspartate, TM 11 tyrosine, and TM 12 lysine and aspartate are residues identified which when mutated (or replaced in chimeric constructs) affect ^{3}H-TBZOH binding (*13*−*16*). On the basis of these data, it appears likely that TM 1/2, TM 7/8, and TM 10−12 together form the core of VMAT.

10), leading to a reduction in [^{3}H]serotonin transport assessed at linear range time points (Figure 4B). Interestingly, a similar reduction in [^{3}H]serotonin transport was observed in the presence of 100 mM DTT. Further, Cys 1 and Cys 5 appeared the most likely candidates for a disulfide bond, since they are the only non-TM pair of cysteines which, if disulfide bound, would produce the result obtained in Figure 3. As experimental confirmation of this hypothesis, replacement of either Cys 1 or Cys 5 eliminated the DTT-reversible covalent bond which tethered the thrombin-cleaved VMAT2 together in the absence of DTT (Figure 5), leading to the conclusion that Cys 1 (Cys 126) and Cys 5 (Cys 333) are the cysteine pair involved in the observed disulfide bond (Figure 6A). We cannot rule out the possibility that there are additional disulfide bonds in VMAT2. Disulfide bonds between Cys 2 and Cys 3 would not be detected by this approach, since they are located on the same side of the thrombin cleavage site. Likewise, disulfide bonds between Cys 4, 6, 7, 8, 9, and 10 would not be detected. However, there cannot be additional disulfide bonds present in VMAT2 between cysteines on opposite sides of loop 6/7 (the thrombin cleavage site), since removing either Cys 1 or Cys 5 results in the complete generation of the transporter halves, with little or no intact VMAT2, under nonreducing conditions. The positions of Cys 1 and Cys 5 near the predicted lumenal interfaces of TM 2 and TM 8 suggest that these two TM segments are likely to be very close to each other in the tertiary structure of the protein. Taken together with photoaffinity labeling data indicating a juxtaposition of TM 1 with TM 10/11 (*20*), ion pair data indicating a juxtaposition of TM 2 and TM 11 (*19*), ^{3}H-TBZOH protectable MTSEA inhibition of ligand binding at Cys 8 in TM 11 (*18*), and mutagenesis and chimera data indicating an involvement of TM 1/2, loop 7/8, and TM 10−12 in TBZ binding (*13*−*17*), we hypothesize that the N- and C-terminal regions, together with the central region (TMs 1/2, 7/8, and 10−12), form the core of the folded VMAT2 structure (Figure 6B).

In transmembrane proteins localized to intracellular vesicles (including VMAT), the lumenal side of the transporter corresponds to the extracellular side of plasma membrane receptors or transporters. The experiments herein presented involved expression of human VMAT2 in a commonly used but heterologous cell line (COS-7). Future studies remain to examine Cys 1−Cys 5 disulfide bond formation in neuronal or neuroendocrine cells. Intracellular vesicle and protein trafficking studies have demonstrated that, in the process of transporter maturation and vesicular recycling, VMAT2 is transiently present at the cell membrane with its lumenal face oriented extracellularly (*7*, *34*). This suggests a possible location where disulfide bond formation might occur in neurons, as part of the transporter maturation process. In fact, the small amount of thrombin-cleaved VMAT2 (loop 6/7 thrombin construct) present in the absence of DTT (Figure 3, lane 4) may represent a population of VMAT2 that has not fully matured although this is speculative and it cannot be ruled out that the small amount of cleaved VMAT2 in the absence of DTT represents a population of improperly folded VMAT2 molecules.

There are a number of previously reported examples of transmembrane proteins with naturally occurring, functionally important disulfide bonds between cysteines in extracellular or lumenal loop regions. A disulfide bond between Cys 110 and Cys 187 in the rhodopsin intradiscal (lumenal) domain (*22*) has been extensively studied and recently confirmed by X-ray crystallography (*35*). Two disulfide bonds appear present in the extracellular domain of the β_2-adrenergic receptor (*23*−*25*), which shares with VMAT2 the functional feature of monoamine binding. On the basis of mutagenesis, uptake, and chemical derivatization studies, the plasma membrane serotonin transporter (SERT, which shares with VMAT2 the functional feature of serotonin transport) appears to have a disulfide bond between cysteines 200 and 209 (both within the large extracellular loop) (*28*, *29*). A particularly relevant comparison may be made with the 12-TM bacterial

Tn10 metal tetracycline proton antiporter, which shares a predicted 12-TM topology and proton antiport mechanism with VMAT2. While Tn10 does not naturally have cysteines in periplasmic loop 1/2 and loop 7/8 (corresponding to the loops containing Cys 1 and Cys 5 in VMAT2), it was demonstrated that a cysteine pair with one cysteine placed in each of these two loops can be oxidized to form a disulfide bond. In the same study (serving as a control), nine other pairs of cysteines positioned in various loops did not form disulfide bonds (*31*). From this demonstration of proximity of loop 1/2 and loop 7/8 by disulfide bond formation, it appears likely that the functional similarity between the proton antiporters VMAT2 and Tn10 will also be reflected in some aspects of structural similarity between these transporters.

Cys 1 and Cys 5, identified as the two cysteines involved in the disulfide bond, are present at the same positions in human, rat, mouse, and bovine VMAT2 and in human and rat VMAT1. This suggests that an important role in maintaining transporter stability is not restricted to human VMAT2 alone but is present throughout mammalian VMATs. If failure to form the disulfide bond resulted in less efficient transport activity (as suggested by our data), one might expect a variety of neurochemical changes, consistent with evidence from studies on VMAT2 heterozygous knockout mice with one-half the normal amount of VMAT2 activity which indicates that a 50% reduction in transport activity leads to correspondingly lower brain levels of monoamine, with enhanced sensitivity to the neurotoxic and certain other effects of abused drugs (*4*−*6*).

In summary, we have identified a disulfide bond between functionally important lumenal cysteines (Cys 126 and Cys 333) in human VMAT2. This provides an important new insight into VMAT2 structure and function and is one of only a few biochemical demonstrations of structural information for this transporter to date. Recognition of a Cys 1−Cys 5 disulfide bond will be essential in future intramolecular cross-linking studies between engineered cysteine pairs. In the background of these constructs (containing engineered thrombin sites and devoid of either Cys 1 or Cys 5), such experiments should prove useful in obtaining additional structural information concerning human VMAT2.

ACKNOWLEDGMENT

We thank Dr. Robert H. Edwards (Departments of Neurology and Psychiatry, University of California, San Francisco) for providing a human VMAT2 cDNA.

REFERENCES

1. Stern-Bach, Y., Greenberg-Ofrath, N., Flechner, I., and Schuldiner, S. (1990) *J. Biol. Chem. 265*, 3961−3966.
2. Liu, Y., Peter, D., Roghani, A., Schuldiner, S., Prive, G. G., Eisenberg, D., Brecha, N., and Edwards, R. H. (1992) *Cell 70*, 539−551.
3. Erickson, J. D., Eiden, L. E., and Hoffman, B. J. (1992) *Proc. Natl. Acad. Sci. U.S.A. 89*, 10993−10997.
4. Fon, E. A., Pothos, E. N., Sun, B. C., Killeen, N., Sulzer, D., and Edwards, R. H. (1997) *Neuron 19*, 1271−1283.
5. Takahashi, N., Miner, L. L., Sora, I., Ujike, H., Revay, R. S., Kostic, V., Jackson-Lewis, V., Przedborski, S., and Uhl, G. R. (1997) *Proc. Natl. Acad. Sci. U.S.A. 94*, 9938−9943.
6. Wang, Y. M., Gainetdinov, R. R., Fumagalli, F., Xu, F., Jones, S. R., Bock, C. B., Miller, G. W., Wightman, R. M., and Caron, M. G. (1997) *Neuron 19*, 1285−1296.
7. Liu, Y., Krantz, D. E., Waites, C., and Edwards, R. H. (1999) *Trends Cell Biol. 9*, 356−363.
8. Liu, Y., and Edwards, R. H. (1997) *Annu. Rev. Neurosci. 20*, 125−156.
9. Itokawa, K., Sora, I., Schindler, C. W., Itokawa, M., Takahashi, N., and Uhl, G. R. (1999) *Brain Res. Mol. Brain Res. 71*, 354−357.
10. Eiden, L. E. (2000) *FASEB J. 14*, 2396−2400.
11. Erickson, J. D., and Varoqui, H. (2000) *FASEB J. 14*, 2450−2458.
12. Merickel, A., Rosandich, P., Peter, D., and Edwards, R. H. (1995) *J. Biol. Chem. 270*, 25798−25804.
13. Steiner-Mordoch, S., Shirvan, A., and Schuldiner, S. (1996) *J. Biol. Chem. 271*, 13048−13054.
14. Peter, D., Vu, T., and Edwards, R. H. (1996) *J. Biol. Chem. 271*, 2979−2986.
15. Finn, J. P., and Edwards, R. H. (1997) *J. Biol. Chem. 272*, 16301−16307.
16. Finn, J. P., and Edwards, R. H. (1998) *J. Biol. Chem. 273*, 3943−3947.
17. Erickson, J. D. (1998) *Adv. Pharmacol. 42*, 227−232.
18. Thiriot, D. S., and Ruoho, A. E. (2001) *J. Biol. Chem. 276*, 27304−27315.
19. Merickel, A., Kaback, H. R., and Edwards, R. H. (1997) *J. Biol. Chem. 272*, 5403−5408.
20. Sievert, M. K., and Ruoho, A. E. (1997) *J. Biol. Chem. 272*, 26049−26055.
21. Sievert, M. K., Thiriot, D. S., Edwards, R. H., and Ruoho, A. E. (1998) *Biochem. J. 330* (Part 2), 959−966.
22. Davidson, F. F., Loewen, P. C., and Khorana, H. G. (1994) *Proc. Natl. Acad. Sci. U.S.A. 91*, 4029−4033.
23. Noda, K., Saad, Y., Graham, R. M., and Karnik, S. S. (1994) *J. Biol. Chem. 269*, 6743−6752.
24. Moxham, C. P., Ross, E. M., George, S. T., and Malbon, C. C. (1988) *Mol. Pharmacol. 33*, 486−492.
25. Dohlman, H. G., Caron, M. G., DeBlasi, A., Frielle, T., and Lefkowitz, R. J. (1990) *Biochemistry 29*, 2335−2342.
26. Wolin, C. D., and Kaback, H. R. (2000) *Biochemistry 39*, 6130−6135.
27. Kwaw, I., Sun, J., and Kaback, H. R. (2000) *Biochemistry 39*, 3134−3140.
28. Chen, J. G., Liu-Chen, S., and Rudnick, G. (1997) *Biochemistry 36*, 1479−1486.
29. Sur, C., Schloss, P., and Betz, H. (1997) *Biochem. Biophys. Res. Commun. 241*, 68−72.
30. Loo, T. W., and Clarke, D. M. (2000) *J. Biol. Chem. 275*, 5253−5256.
31. Kubo, Y., Konishi, S., Kawabe, T., Nada, S., and Yamaguchi, A. (2000) *J. Biol. Chem. 275*, 5270−5274.
32. Tamura, N., Konishi, S., Iwaki, S., Kimura-Someya, T., Nada, S., and Yamaguchi, A. (2001) *J. Biol. Chem. 276*, 20330−20339.
33. Martin, T. F. (1989) *Methods Enzymol. 168*, 225−233.
34. Tan, P. K., Waites, C., Liu, Y., Krantz, D. E., and Edwards, R. H. (1998) *J. Biol. Chem. 273*, 17351−17360.
35. Palczewski, K., Kumasaka, T., Hori, T., Behnke, C. A., Motoshima, H., Fox, B. A., Le Trong, I., Teller, D. C., Okada, T., Stenkamp, R. E., Yamamoto, M., and Miyano, M. (2000) *Science 289*, 739−745.

BI015779J